

Trends and Spatio-Temporal Variability of Summer Mean and Extreme Precipitation Events across South Korea for 1973-2022

Hye-Ryeom Kim¹, Mincheol moon², Junghee Yun², Kyung-Ja Ha³, Hanh Nguyen⁴, Chang-Hoi Ho⁵, Doo-Sun Park⁶, Minha Choi⁷, Jason Otkin⁸, Won-Ho Nam⁹, Ramesh Kripalani¹⁰, Kyung Hwa Cho¹¹, and Richard Cooke¹²

¹Pusan National University, Busan, Republic of Korea

²Pusan National University

³Center for Climate Physics, Institute for Basic Science (IBS)

⁴Centre for Australian Weather and Climate Research

⁵Seoul National University

⁶Kyungpook National University

⁷Sungkyunkwan University

⁸U. Wisconsin

⁹Hankyong National University

¹⁰Indian Institute of Tropical Meteorology

¹¹Ulsan National Institute of Science and Technology

¹²University of Illinois at Urbana Champaign

December 10, 2022

Abstract

Climate change has altered the frequency, intensity, and timing of mean and extreme precipitation events. Extreme precipitation has caused tremendous socio-economic losses and displays strong regional variability. Although many previous studies have addressed daily extreme precipitation, hourly extreme rainfall still needs to be thoroughly investigated. In this study, we investigated the trends, spatio-temporal variability, and long-term variations in mean and extreme precipitation over South Korea using daily and hourly observational data. During the past 50 years (1973–2022), there has been a notable escalation in maximum hourly precipitation, although the boreal summer mean precipitation has increased only marginally. Regionally, an increase in mean and extreme rainfall occurred in the northern part of the central region. Moreover, increased intensity and frequency of extreme precipitation have contributed more to the total summer precipitation in recent years. Our findings provide scientific insights into the progression of extreme summer precipitation events in South Korea.

Hosted file

951646_0_art_file_10517052_rmjr88.docx available at <https://authorea.com/users/565241/articles/612256-trends-and-spatio-temporal-variability-of-summer-mean-and-extreme-precipitation-events-across-south-korea-for-1973-2022>

Hosted file

951646_0_supp_10517053_rmjr89.docx available at <https://authorea.com/users/565241/articles/612256-trends-and-spatio-temporal-variability-of-summer-mean-and-extreme-precipitation-events-across-south-korea-for-1973-2022>

1
2 **Trends and Spatio-Temporal Variability of Summer Mean and Extreme**
3 **Precipitation Events across South Korea for 1973–2022**
4

5 **Hye-Ryeom Kim^{1,3}, Mincheol Moon^{2,4}, Junghee Yun^{3,4}, and Kyung-Ja Ha^{1,2,3,4*}**

6 ¹BK21 School of Earth and Environmental Systems, Pusan National University, Busan, Republic
7 of Korea.

8 ²Department of Climate System, Pusan National University, Busan, Republic of Korea.

9 ³Department of Atmospheric Sciences, Pusan National University, Busan, Republic of Korea.

10 ⁴Center for Climate Physics, Institute for Basic Science, Busan, Republic of Korea.

11
12 Corresponding author: Kyung-Ja Ha (kjha@pusan.ac.kr)

13
14 **Key Points:**

- 15 • Observational data are invaluable in studying extreme precipitation events.
16 • Extreme precipitation increased in 1973–2022, with the hourly-maximum precipitation
17 showing a statistically significant increase.
18 • Extreme precipitation has a major effect on the summer rainfall in South Korea.
19

20 **Abstract**

21 Climate change has altered the frequency, intensity, and timing of mean and extreme
22 precipitation events. Extreme precipitation has caused tremendous socio-economic losses and
23 displays strong regional variability. Although many previous studies have addressed daily
24 extreme precipitation, hourly extreme rainfall still needs to be thoroughly investigated. In this
25 study, we investigated the trends, spatio-temporal variability, and long-term variations in mean
26 and extreme precipitation over South Korea using daily and hourly observational data. During
27 the past 50 years (1973–2022), there has been a notable escalation in maximum hourly
28 precipitation, although the boreal summer mean precipitation has increased only marginally.
29 Regionally, an increase in mean and extreme rainfall occurred in the northern part of the central
30 region. Moreover, increased intensity and frequency of extreme precipitation have contributed
31 more to the total summer precipitation in recent years. Our findings provide scientific insights
32 into the progression of extreme summer precipitation events in South Korea.

33

34 **Plain Language Summary**

35 Climate change affects both mean and extreme precipitation events. This leads to changes in the
36 frequency, intensity, and timing of extreme rainfall events. Extreme precipitation is inextricably
37 linked to our human livelihoods and has the potential to cause substantial socioeconomic losses.
38 In addition, there are large regional differences between these events. Although many previous
39 studies have examined daily extreme precipitation, hourly extreme rainfall remained unclear.
40 Here we investigated the trends, spatio-temporal variability, and long-term variations in mean
41 and extreme precipitation across South Korea using daily and hourly observational data. It was
42 important to note that hourly maximum precipitation was significantly intensified, whereas the
43 boreal summer mean precipitation displayed a slight increase over the past 50 years (1973–
44 2022). In terms of spatial distribution, the northern part of the central region experienced an
45 increase in mean and extreme rainfall. Also, increased intensity and frequency of extreme
46 precipitation have played key roles in the summertime total precipitation in recent years. Our
47 findings provide a scientific background for understanding changes in summer extreme rainfall
48 events in South Korea.

49

50 **1 Introduction**

51 Climate change has a significant impact on the Earth system. Globally, total human-
52 induced surface air temperature increased by approximately 1.07 °C (0.8 °C to 1.3 °C) from
53 1850 to 2019 (IPCC, 2022). In tandem with rising temperatures, worldwide mean precipitation
54 tends to increase (Allen & Ingram, 2002; Held & Soden, 2006). The frequency of heavy rainfall
55 has increased considerably since 1951, and it varies strongly between regions and subregions
56 (IPCC, 2022). Light precipitation events decreased in frequency, whereas heavy precipitation
57 events increased in frequency and intensity (Trenberth et al., 2003; Alexander et al., 2006;
58 Kharin et al., 2007; Allan & Soden, 2008; O’Gorman & Schneider, 2009; Min et al., 2011; Chou
59 et al., 2012; Ha et al., 2020). The Intergovernmental Panel on Climate Change (IPCC) also
60 pointed out that climate change could affect the frequency, intensity, and timing of extreme
61 events such as heatwaves, droughts, tropical cyclones, and extreme rainfall events (IPCC, 2022).
62 As one of the most hazardous extreme phenomena, extreme rainfall events bring considerable

63 damage, resulting in secondary disasters including landslides and flash floods (Dave et al., 2021;
64 Kim et al., 2021; Meyer et al., 2021; Ning et al., 2021). Extreme rainfall has a severe impact on
65 human life, ecosystems, and the social economy of agriculture, causing colossal socioeconomic
66 losses. Therefore, it is essential to understand extreme rainfall events.

67 Compared to the global mean surface warming, South Korea has experienced
68 considerably greater surface warming because of the complex influence of several climate
69 variabilities along the northeastern coast of Asia (Jung et al., 2002; An et al., 2011). In terms of
70 linear trends, the local temperatures have risen by 1.90 °C (1912–2014), 1.35 °C (1954–2014),
71 and 0.99 °C (1973–2014), which are 1.4–2.6 times greater than the global land mean temperature
72 increases (Park et al., 2017). Regarding global warming, particularly for the Korean Peninsula
73 (KP), a growing number of previous studies proposed that the frequency and intensity of extreme
74 weather events (i.e., extreme precipitation events, droughts, heat waves, and tropical cyclones)
75 have increased over the past few decades (Kim et al., 2012; Lee et al., 2012; Min et al., 2015; Ha
76 et al., 2020; Park et al., 2021; Seo et al., 2021). This summer, the metropolitan area endured
77 particularly heavy torrential rain and flooding. In Seoul, an hourly downpour of 141.5 mm/hr
78 was recorded, which was the heaviest hourly precipitation breaking the record in 80 years (Baek
79 & Yeung, 2022). In addition, this event surpassed 381.5 mm, which was the heaviest daily
80 precipitation recorded in the past 102 years. At least 14 people died as a result of heavy rainfall,
81 and the total sum of the damage was estimated to exceed USD 50M. Several studies have
82 investigated the changes in mean and extreme rainfall in South Korea (Ho et al., 2003; Jung et al.,
83 2011; Baek et al., 2017; Azam et al., 2018). Most of these studies focused on daily extreme
84 precipitation, therefore, our understanding of hourly extreme rainfall events is insufficient.
85 However, hourly extreme precipitation should be highlighted because it can induce great damage,
86 as we have already experienced.

87 As one of the primary factors of heavy rainfall events, the Changma and typhoons greatly
88 impact extreme precipitation, whereas the East Asian summer monsoon has a major effect on the
89 rainy season (Lee et al., 2017). The Changma is most active between early July and early
90 September, with the first Changma starting in late June and ending in late July (Seo et al., 2011;
91 Park et al., 2015). In addition, the second Changma is mainly associated with typhoons in late
92 summer, and typhoons intensively affect the KP in July, August, and September (Lee et al.,
93 2017; Moon & Ha, 2021). Heavy rainfall in the KP during the boreal summer needs to be
94 investigated because the sub-seasonal variability is very large, even during summer.

95 On the other hand, it is necessary to understand long-term variations and trends in mean
96 and extreme precipitation in water resource and flood risk management (Moberg et al., 2006; Ha
97 et al., 2009; Pei et al., 2017; Kim & Ha, 2021; Wang et al., 2021; Hu et al., 2022; Ryan et al.,
98 2022). Ensemble empirical mode decomposition (EEMD) method is employed to appropriately
99 reflect nonlinear responses to global warming and urbanization (Yun et al., 2018; Jeong et al.,
100 2022). Hu et al., (2022) revealed that the extreme precipitation on the Tibetan Plateau and its
101 surrounding areas is strongly correlated with the strength of the Indian Ocean and Western
102 Pacific warm pools through the multi-time-scale analysis.

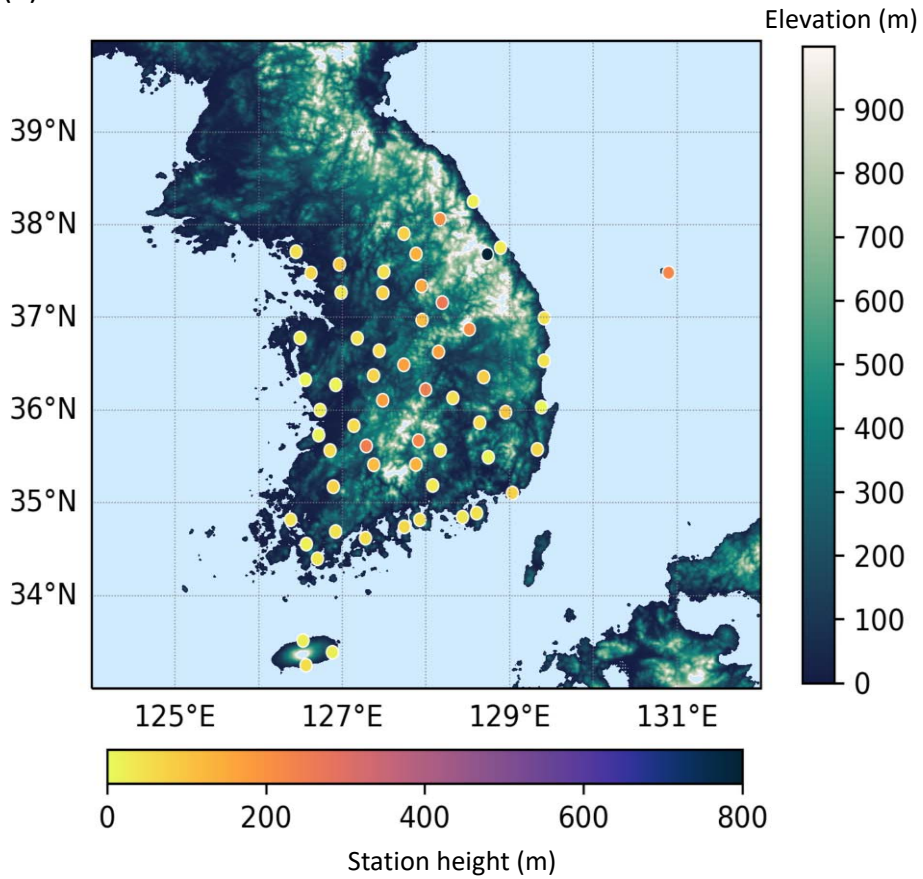
103 Consequently, the purpose of this study was as follows: (1) to analyze the trends of
104 extreme precipitation in terms of hourly and daily time scales, as well as their spatial patterns
105 over South Korea; (2) to focus on long-term variations in the mean temperature and extreme
106 precipitation, as well as their relationships with EEMD methods; and (3) to identify the recent
107 changes in major spatio-temporal distributions of summertime precipitation.

108 **2 Data and Methods**

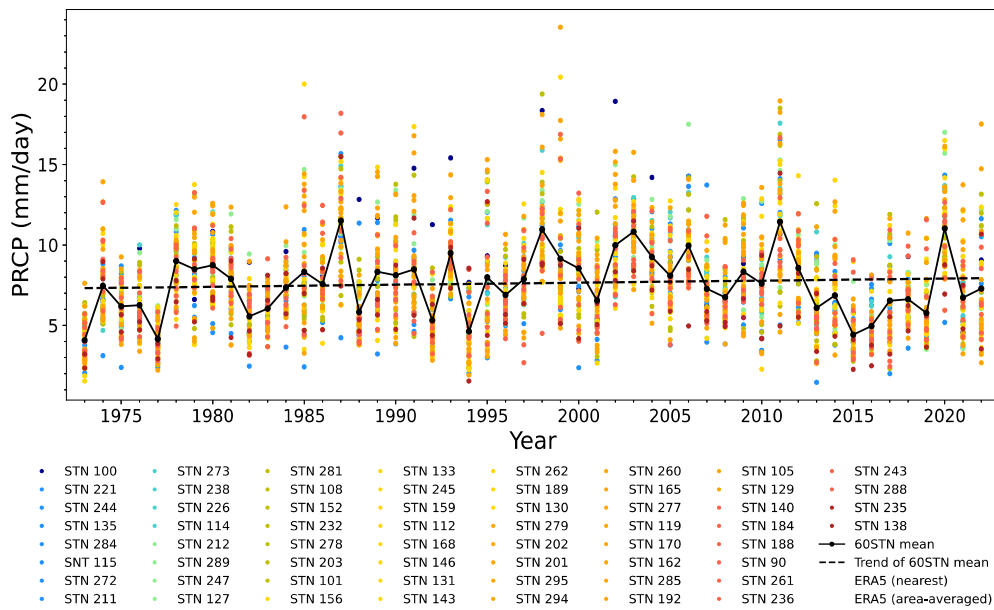
109 **2.1 Data**

110 We used daily mean precipitation, 1-hour maximum precipitation, and daily mean
111 temperature from the Automated Surface Observing System (ASOS) for the investigation of
112 trends and variability in Korean summer rainfall from 1973 to 2022. Sixty stations out of a total
113 of 103 stations were selected, encompassing the entire analysis period (Figure 1a). The months
114 of June–July–August (JJA) are regarded as the boreal summer. Hourly precipitation data were
115 obtained from the European Center for Medium-Range Weather Forecasts reanalysis version 5
116 (ERA5; Hersbach et al., 2020). We adjusted the time in line with Korea Standard Time (KST)
117 owing to the time difference between the Universal Time Coordinate (UTC) and KST. For the
118 ERA5 reanalysis data, the area-averaged precipitation and nearest grid point precipitation were
119 compared to the ASOS total station mean precipitation. Instead of area-averaged precipitation,
120 the nearest grid point precipitation corresponded more closely with the ASOS. However, since
121 the late 1990s, the ERA5 dataset has tended to underestimate the JJA mean precipitation from
122 the ASOS (Figure 1b). In particular, when the JJA mean precipitation was at its peak, ERA5 data
123 could not match the observation. A heavy rainfall event is typically a localized event occurring in
124 a small area. Therefore, ERA5, which had a spatial resolution of approximately 30km, was not
125 sufficient to simulate these peak events in observation. This was consistent with that of Borodina
126 et al., (2017) and highlighted the importance of observational data in studying localized heavy
127 rainfall events. In terms of the topography, the ETOPO1 dataset was selected (Amante & Eakins,
128 2009).

(a) Locations of ASOS stations



(b) JJA daily mean precipitation



130 **Figure 1.** (a) Topographical sketch map of South Korea with 60 ASOS stations (circles, bottom
 131 colored bar). The shading displays the topographic elevation (upper-right colored bar). (b)
 132 Interannual variability in summertime (JJA) daily precipitation at each station over the past 50
 133 years (1973–2022). The solid black line represents the JJA mean precipitation of all stations, and
 134 its trend is indicated via a black dashed line. For the ERA5 dataset, the nearest grid point of each
 135 station (solid dark olive-green line) and area-averaged value (solid yellow-green line) are also
 136 exhibited.

137

138 2.2 Extreme Indices

139 Five indices derived from the Expert Group on Climate Change Detection and Indices
 140 (ETCCDI) were calculated to describe the features of extreme precipitation (Table S1). A wet
 141 day indicated that the daily precipitation amount was more than 1mm (Yao et al., 2008; Kim et
 142 al., 2013). The total precipitation (PRCPTOT) was the sum of precipitation on wet days.
 143 Extremely wet day total precipitation denoted instances where the daily precipitation exceeded
 144 the 95th and 99th percentiles of the wet day precipitation (R95p, R99p); this was calculated during
 145 the summer. In addition, to compare the changes in summertime precipitation, we divided the 50
 146 years into two periods: 1973–1992 (P1, reference period) and 2003–2022 (P2), and calculated
 147 each percentile value for the reference period. For frequency, we used the number of heavy
 148 precipitation days when the daily precipitation amount was more than 20mm (R20mm) and the
 149 number of dry days when the daily precipitation was less than 1mm. We defined the number of
 150 days with R95p and R99p as R95pF and R99pF, respectively. The hourly extreme precipitation
 151 index (RX1H) was defined as the maximum 1-hour precipitation; this index was used to focus on
 152 heavy downpours in a short period of time. In Section 3.3, we selected a high-population group
 153 with a population of more than 1,000,000 and a low-population group with a population of less
 154 than 50,000 in order to examine the effects of urbanization on extreme precipitation (Table S2).

155

156 2.3 Ensemble Empirical Mode Decomposition (EEMD)

157 An improved noise-assisted data analysis method, Ensemble Empirical Mode
 158 Decomposition (EEMD), decomposes the original signals ($x(t)$) into a finite number (N) of
 159 independent signals with periodicity ($C_i(t)$, $i = 1, 2, 3, \dots, n$) and a residual linear or nonlinear
 160 trend ($R(t)$) (Wu & Huang, 2004, 2009).

161

$$162 \quad x(t) = \sum_{i=1}^n C_i(t) + R(t) \quad (1)$$

163

164 Here, the standard deviation of the added noise series and the ensemble number for EEMD were
 165 entered as 0.2 and 200, respectively.

166

167 2.4 Extended Empirical Orthogonal Function (EEOF)

168 The Extended Empirical Orthogonal Function Analysis (EEOF) was employed in
 169 conjunction with reanalysis data to analyze the temporal evolution of the principal spatial
 170 structure. Several previous studies have applied EEOF to investigate the evolution of the

171 substructure (Chen & Harr, 1993; Kim et al., 2008). Using the EEOF analysis, we interpreted the
 172 substructure as the propagation or evolution of the sub-seasonal mode over time of the first
 173 substructure of the function. The eigenvector and eigenfunction for an atmospheric variable,
 174 $\mu_{ij'}^{(n)}$, were as follows:

$$175 \alpha_{il}^{(n)} = \sum_{j'=1}^{J'} \mu_{ij'}^{(n)} \Psi_{j'l} \quad (2)$$

177 where i indicates the space, j denotes the time, j' indicates the time in the window, and n
 178 represents the number of windows. $\Psi_{j'l}$ is a function of temporal variation, and α_{il} is a window-
 179 averaged space structure with the l -th eigenfunction serving as the weight. In a previous study, a
 180 window size of 20 days was used to focus on quasi-stationary properties (Kim et al., 2008). In
 181 this study, we set the window size (substructure) as the minimum sub-seasonal time scale (2
 182 weeks) with a lag of 6 days to analyze the evolution of precipitation in the finer sub-seasonal
 183 mode. The number of windows (n in Equation (2)) was 14, from June 1 to August 31.

185

186 3 Results

187 3.1 Boreal Summer Mean and Extreme Precipitation from 1973 to 2022

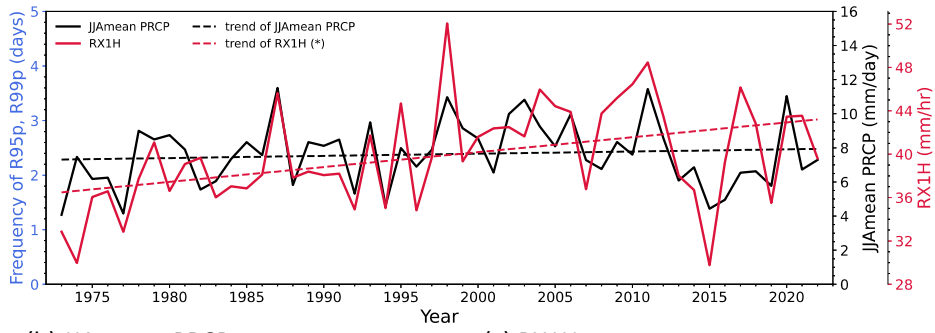
188 To determine the interannual variability (IAV) of the JJA mean daily precipitation, we
 189 calculated the IAV for each station between 1973 and 2022. Figure 1b depicts the IAV of each
 190 ASOS station, the total station mean as well as area-averaged, and the closest grid point values of
 191 ERA5. The IAV of the JJA mean precipitation shows large differences among stations.
 192 Similarly, in Figure 2a (grey shading), the JJA mean precipitation exhibits large spatial
 193 variability among the stations. This result supported the notion that precipitation in South Korea
 194 displayed strong spatial variability (Jung et al., 2011). In addition, the station mean of JJA mean
 195 precipitation exhibited a slightly increasing trend of 0.65 mm/day over 50-year period, but it was
 196 not statistically significant. Spatially, 80% of the total stations (48 of 60 stations) presented an
 197 increasing trend in JJA mean precipitation, whereas 20% displayed a decreasing trend, which
 198 was not significant (Figure 2b). Specifically, 20% of total stations (12 of 60 stations) showed a
 199 greater increasing trend (above 1.5mm/day) over the 50-year period, and most of these stations
 200 were concentrated in the northern part of the central region near 38°N and certain coastal regions
 201 such as Geoje and Busan.

202 Five indices were calculated as indicators of extreme precipitation: RX1H, R95p, R99p,
 203 R95pF, and R99pF. These indices showed an increasing trend for the 50-year period, but only
 204 two had significant increasing trends at a 90% significance level. Figure 2a displays the IAV and
 205 trends for the extreme indices from 1973 to 2022. While JJA mean precipitation showed a very
 206 slight increase (0.65 mm/day/50 yrs), RX1H presented a very clear increasing trend (7 mm/hr/50
 207 yrs) at a 99% significance level. The linear trends of R95p (R99p) and R95pF (R99pF) were 60.5
 208 mm/50 yrs (37 mm/50 yrs) and 0.5 days/50 yrs (0.2 days/50 yrs) for the same period,
 209 respectively. Figures 2c–2g show the spatial distribution of the linear trend for each extreme
 210 precipitation index. For RX1H, 50 (10) stations, which accounted for 83.3% (16.7%) of the total
 211 stations, showed an increasing (decreasing) trend over the past five decades. Twelve stations
 212 (20%) had a significant increasing trend for RX1H (Figure 2c). Most of the significant stations

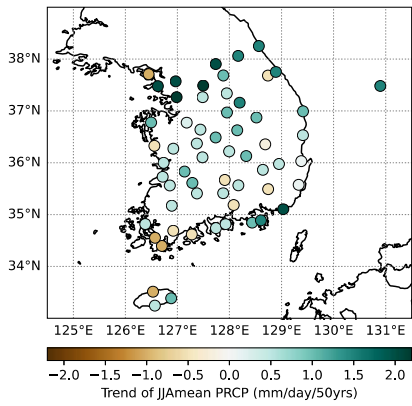
213 were concentrated in the northern portion of the central region, along the southern coast of Korea.
214 Some stations, such as Imsil and Gumi, were located in inland regions. For R95p, 47 (13)
215 stations, which equate to 78.3% (21.7%), showed increasing (decreasing) trends, and seven
216 stations (approximately 13%) showed significant increasing trends (Figure 2d). In addition to
217 RX1H, the majority of the significant regions were located in the northern portion of the central
218 region. The frequency of R95p occurred more (less) frequently at 43 (17) stations, comprising
219 71.7% (28.3%) of total stations. Specifically, six stations (10%) displayed increasing trends in
220 R95pF, and their locations were identical to those of R95p, except for one less station (Figure 2e).
221 An increasing (decreasing) trend for R99p was observed at 46 (14) stations, comprising 76.7%
222 (23.3%) of total stations. Specifically, only 3 (5%) stations, namely Incheon, Inje, and Ulleungdo
223 Island, exhibited a significant increasing trend (Figure 2f). Likewise, the frequency of R99p
224 tended to increase (decrease) at 45 (15) stations, with 75% (25%) and six stations (10%)
225 experiencing significant increases. These stations are primarily located in the northern and
226 several coastal regions (Figure 2g). In general, extreme precipitation intensified in the northern
227 portion of the South and certain coastal regions. The exception was the inland basin of Gumi,
228 which also experienced significant increases in RX1H, R95p, and R95pF.

229 The changes in JJA mean rainfall and each extreme precipitation index between the P1
230 and P2 revealed the evolution of daily precipitation in South Korea over the past two decades
231 (Figure S1). The increase in the JJA mean precipitation rate was 6.71%. Given that the JJA mean
232 precipitation was 7.63 mm/day for 50-years period, higher summer precipitation was indicated in
233 P2 with a value of 7.72 mm/day, whereas 7.24 mm/day was depicted in P1. The RX1H increased
234 by 12.28%. In addition, R95p (R95pF) tended to increase by approximately 22.85% (20.91%). A
235 notable increase in R99p (R99pF) was observed, at a rate of 43.23% (47.3%), during P2. In
236 addition, South Korea exhibited salient intraseasonal variability; therefore, there was a need to
237 divide the summer season into monthly segments (Ha & Oh, 2019; Jia et al., 2022; Ren et al.,
238 2022). The monthly average precipitation was the highest in July (8.99 mm/day), followed by
239 August (8.55 mm/day), and June (5.26 mm/day). In P1 and P2, JJA mean precipitation increased
240 in July (P1: 8.63 mm/day, P2: 9.92 mm/day) and August (P1: 7.58 mm/day, P2: 8.46 mm/day),
241 whereas it decreased in June (P1: 5.44 mm/day, P2: 4.68 mm/day). R95p (R95pF) and R99p
242 (R99pF) comprised the largest portions at 40.93% (41.12%) and 42.76% (43.16%) in July,
243 respectively, which was followed by August at 38.04% (34.74%) and 39.15% (35.71%), as well
244 as June at 21.03% (24.14%) and 18.09% (21.13%), respectively, for 1973–2022. The amount and
245 frequency of extreme precipitation were mostly concentrated in July. Comparing P1 and P2, this
246 trend became more pronounced in P2. For P1, R95p (R95pF) was 25.17% (27.52%), 38.21%
247 (38.87%), and 36.62% (33.62%) in June, July, and August, respectively. Similarly, R99p
248 (R99pF) constituted 24.37% (27.52%), 39.31% (39.37%), and 36.32% (33.11%) in June, July,
249 and August, respectively. During P2, R95p (R95pF) accounted for 17.05% (19.81%), 49.78%
250 (49.00%), and 33.17% (31.19%) in June, July, and August, respectively. In the case of R99p
251 (R99pF), 15.27% (18.13%), 54.41% (53.51%), and 30.32% (28.36%) were observed in June,
252 July, and August, respectively. In P2, extreme precipitation decreased in June, with the exception
253 of R99pF. Although these four indices increased in July and August, a much further increase was
254 observed in July. Thus, the ratio of extreme indices appeared to decline in August in P2, whereas
255 there was an increase in extreme rainfall occurs in July.

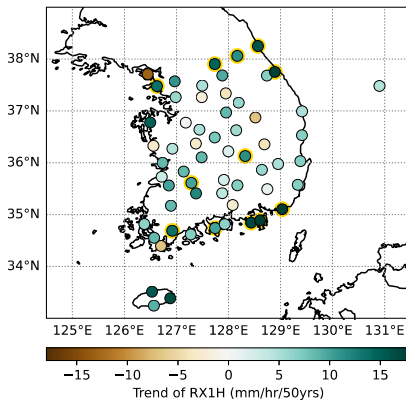
(a) Trend and interannual variability



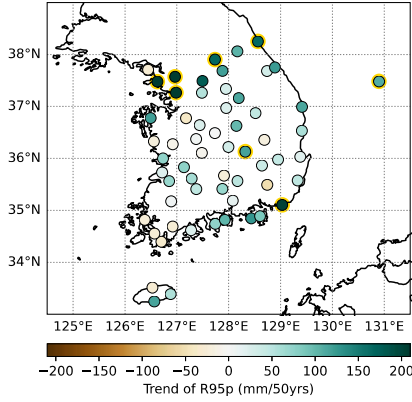
(b) JJA mean PRCP



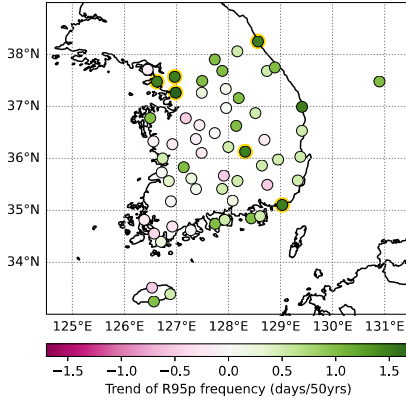
(c) RX1H



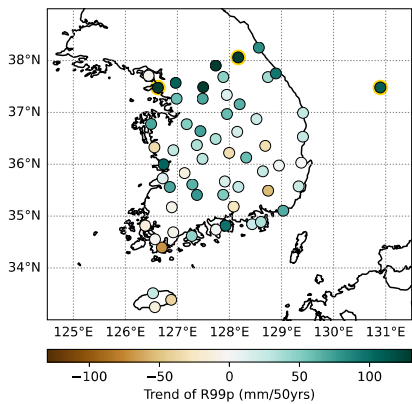
(d) R95p



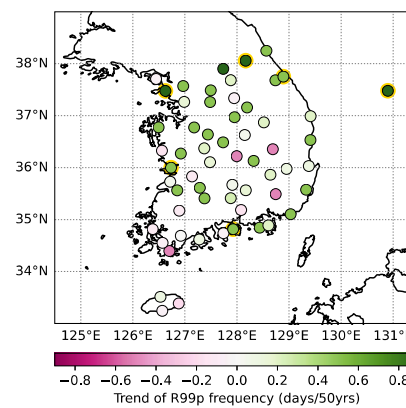
(e) R95pF



(f) R99p



(g) R99pF

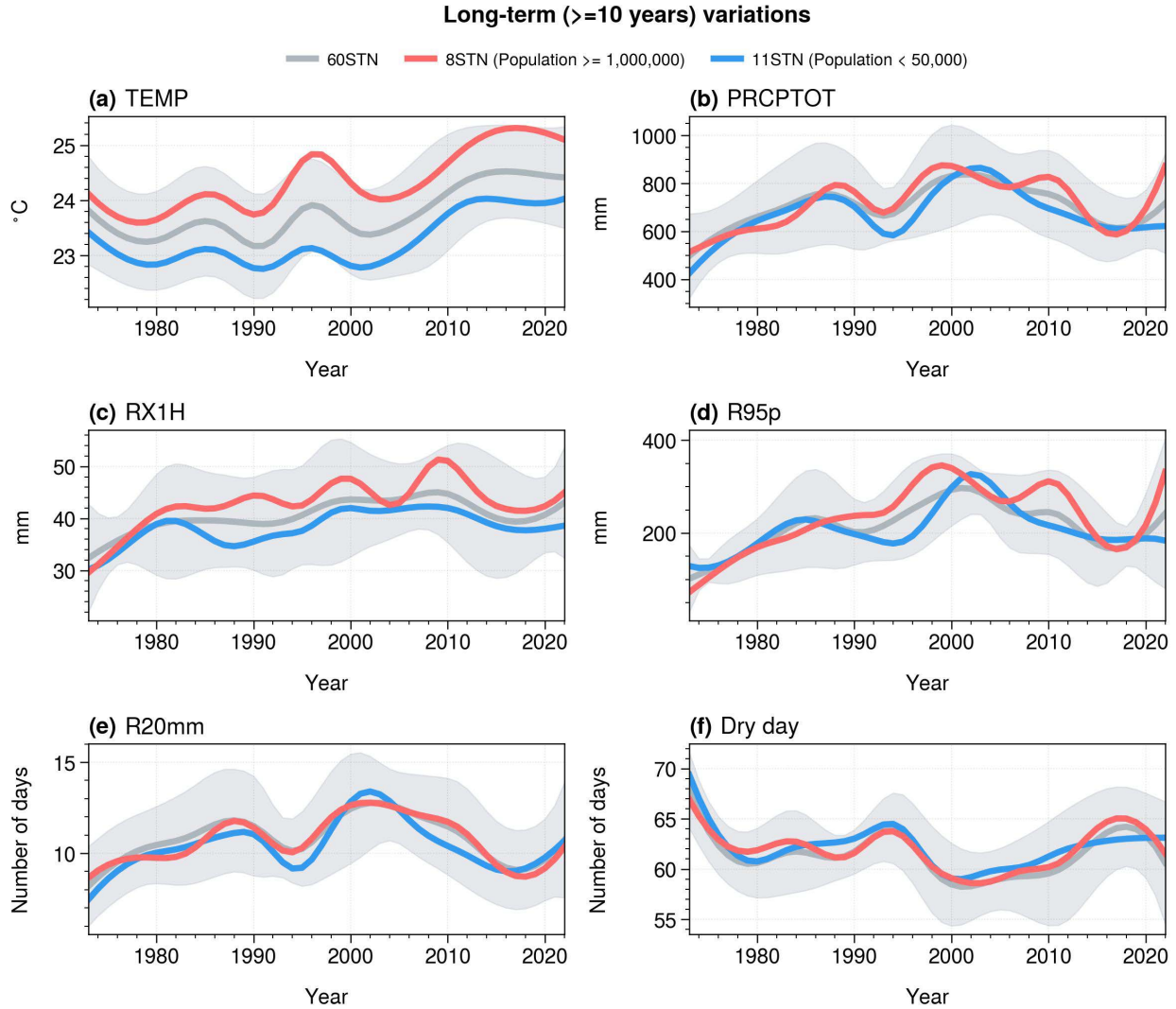


257 **Figure 2.** (a) Time series of boreal summer daily mean precipitation (JJA mean precipitation,
 258 solid black line) with its trend (dashed black line) and spatial variability (grey shading) from
 259 1973 to 2022. Extreme indices, hourly-maximum precipitation (RX1H, solid red line) and its
 260 trend (dashed red line), as well as the frequencies of R95p (R95pF, light sky-blue bar) and R99p
 261 (R99pF, blue bar). The spatial patterns of the trends over the past 50 years are presented in (b)
 262 JJA mean precipitation (mm/day/ 50yrs), (c) RX1H (mm/hr/50 yrs), (d) R95p (mm/50 yrs), (e)
 263 R95pF (days/50 yrs), (f) R99p (mm/50 yrs), (g) R99pF (days/50 yrs). The enclosed yellow
 264 indicates statistical significance at a 90% confidence level.
 265

266 3.2 Long-term Variations in Mean Temperature and Extreme Precipitation Indices

267 The EEMD decomposed the mean temperature and extreme precipitation indices into
 268 four interannual to interdecadal components (C1 to C4) and one residual trend (Table S3). For
 269 1973–2022, C1 and C2 showed approximately 2.8-year and 5.6-year periodic oscillations,
 270 accounting for approximately 55.9% and 20.7% of the total variance, respectively. C3 and C4
 271 show approximately 11.2-year and 28.7-year oscillations and contribute about 10.0% and 4.2%
 272 of the total variance, respectively. The residual trend was 9.1%.

273 To shed light on the long-term changes in the mean temperature and extreme
 274 precipitation indices, we defined long-term variations as the sum of decomposed components
 275 with more than 10 years of mean periods (C3 and C4) and residuals. Higher temperatures were
 276 recorded in high-population regions than in low-population regions (Figure 3a). This result
 277 corresponds to the fact that big cities have experienced greater warming because of rapid
 278 urbanization and population growth since 1973 (Korea Meteorological Administration, 2020).
 279 One salient feature was that long-term changes in mean temperature and PRCPTOT did not
 280 occur simultaneously. The mean temperature increased, with multi-decadal fluctuations entering
 281 a phase higher than the mean temperature (23.7 °C) from the mid-2000s and stabilizing at 24.4 to
 282 24.5 °C after 2010 (Figure 3a). However, PRCPTOT was in a phase higher than the mean
 283 PRCPTOT (698.7 mm) from the mid-1990s to 2010. It peaked at 837 mm in 2002 and decreased
 284 to 613.7 mm in 2017. Since then, it has soared (Figure 3b). RX1H, R95p, and R20mm also
 285 displayed similar features to PRCPTOT (Figures 3c-e), and the dry day was negatively correlated
 286 with PRCPTOT (Figure 3f), indicating that the frequency and intensity of extreme precipitation
 287 contributed significantly to PRCPTOT and implying that the increase in the number of dry days
 288 and the increase in the frequency and intensity of extreme precipitation during the recent years
 289 have greatly influenced the total precipitation in summer. Notably, the long-term changes in
 290 PRCPTOT, RX1H, and R95p appeared to be greater in urbanized areas. This result was
 291 consistent with that of Wang et al., (2021).
 292



293

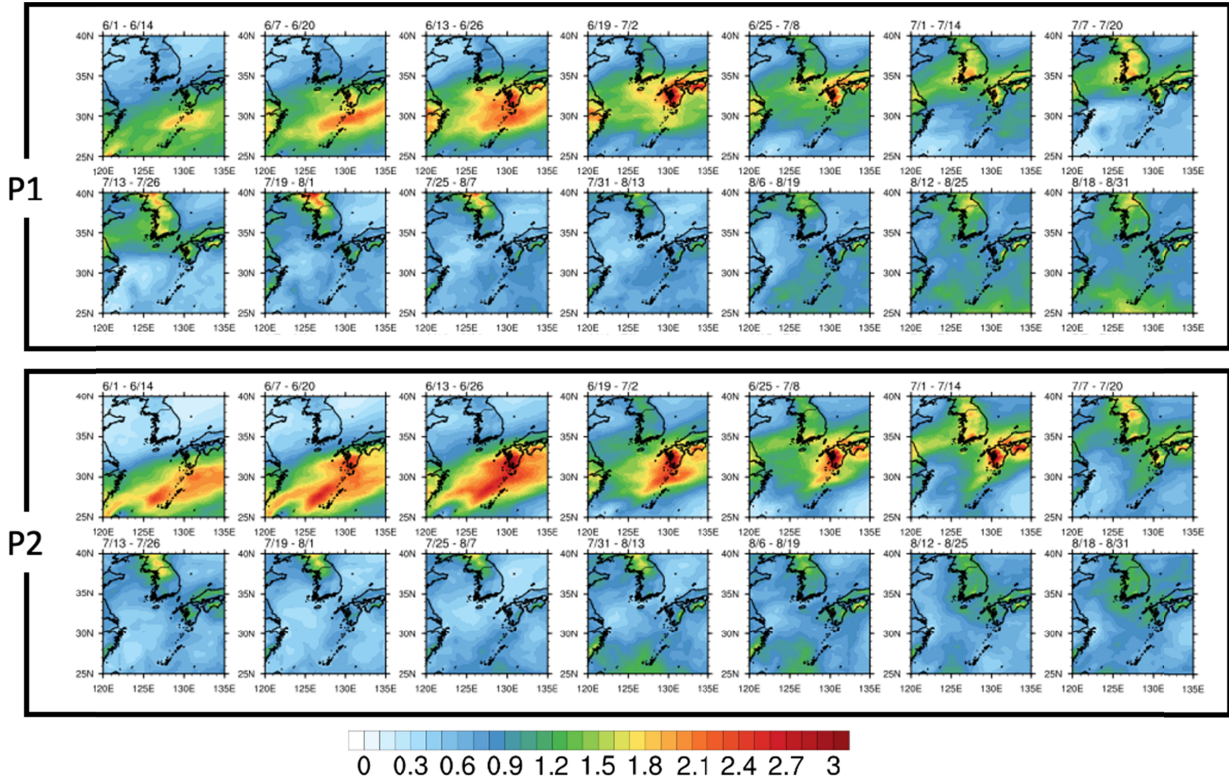
294 **Figure 3.** Long-term variations of (a) mean temperature ($^{\circ}\text{C}$), (b) PRCPTOT (mm), (c) RX1H
 295 (mm), (d) R95p (mm), (e) R20mm (days), and (f) dry day (days) from 1973 to 2022 at 60
 296 stations (grey line); 8 stations had a population of 1 million or more (red line), and 11 stations
 297 with a population of 50000 or less (blue line). Grey-shaded areas represent one standard error of
 298 the mean values from 60 stations. Long-term variations were defined as the sum of decomposed
 299 components with mean periods and residuals exceeding 10 years. 8STN (population
 300 $\geq 1,000,000$): Seoul, Busan, Incheon, Daegu, Daejeon, Gwangju, Suwon, and Ulsan. 11STN
 301 (population $< 50,000$): Uljin, Wando, Hapcheon, Namhae, Jangheung, Yeongdeok, Sancheong,
 302 Boeun, Inje, Imsil, Ulleungdo.

303

304 3.3 Sub-seasonal Modes of Precipitation across East Asia during the Boreal Summer

305 Sub-seasonal evolution is important because the Changma rainband shifts with the
 306 summer monsoon. Especially in recent years, ERA5 data could not exactly describe the IAV;
 307 therefore, we attempted to compare interdecadal changes between P1 and P2. We utilized the
 308 EEOF method on ERA5 daily precipitation over East Asia [120°E – 135°E , 25°N – 40°N] from

309 June 1 to August 31 during P1 and P2, respectively, in order to analyze the sub-seasonal mode
 310 because the characteristics of the rainfall concentrated in summer were variable even within the
 311 season (Figure 4). The first mode of EEOF accounted for 84.9% of the total variance and clearly
 312 demonstrated the spatio-temporal evolution of daily precipitation throughout East Asia.
 313



314 **Figure 4.** The temporal evolution of the spatial distribution of the first EEOF mode of daily
 315 precipitation from June to August for P1 (1973–1992) and P2 (2003–2022).
 316

317
 318 The stationary precipitation core in the Satsunan Islands, which appeared in the first
 319 window (6/1–6/14) near 30°N, developed over time and moved to the KP in the eighth window
 320 (7/13–7/26). The spatial distribution of precipitation revealed a core in the north KP and a weak
 321 signal in the south KP from the ninth window (mid-July) to the 11th window (early August). In
 322 addition to the precipitation that developed locally in the KP, precipitation signals arose south of
 323 30°N in the 12th window. These characteristics appeared in both periods, but the magnitude and
 324 disappearance of the precipitation signals were different between P1 and P2.

325 Compared to the first EEOF mode in P1, a broader and stronger precipitation core
 326 appeared in the Satsunan Islands and Okinawa, and a weaker precipitation signal appeared in the
 327 KP in the first window in P2. Subsequently, the spatio-temporal evolution shifted northward in
 328 the fifth window and rapidly disappeared in the eighth window. The precipitation signal that
 329 developed south of 30°N shifted to the earlier two windows compared to that of P1. In the 13th
 330 and 14th windows, the local precipitation signal located at the KP became weaker compared to
 331 that of P1.

332 This transition from P1 to P2 demonstrated that throughout the recent two decades, the
 333 precipitation core that developed in the early boreal summer (the first window to the fifth
 334 window) became stronger with time, whereas the precipitation core generally weakened in the

335 middle period (after the sixth window). Thus, the climatological sub-seasonal mode of
336 precipitation associated with heavy rainfall in the EA region has recently become stronger and
337 shorter.
338

339 **4 Summary and Discussion**

340 This study analyzed the trend and variability of the summer mean and extreme
341 precipitation from 1973 to 2022. Until the mid-1990s, the ERA5 was similar to the observations.
342 However, since the late 1990s, precipitation from the reanalysis dataset has had a tendency to be
343 underestimated, particularly at the peak of precipitation. This implied that torrential rainfall
344 became more localized, and it was difficult to capture extreme events on a sub-grid scale solely
345 using the reanalysis dataset. Therefore, observational data were invaluable for studying extreme
346 rainfall events. Generally, precipitation indices, in terms of intensity and frequency, showed an
347 increasing trend from 1973 to 2022. One noteworthy result was a significant increase in the
348 hourly-maximum precipitation, whereas the mean precipitation presented a slight increase. In
349 terms of frequency, the number of R99p days became significantly more frequent. Regarding
350 spatial distribution, summer precipitation exhibited greater spatial variability across South Korea.
351 In general, it was illustrated that an increasing trend of mean and extreme precipitation occurred
352 in the northern part of the central region. Additionally, RX1H, R95p, and R95pF increased in
353 some coastal and inland areas.

354 Changes in mean and extreme precipitation were identified in two periods; P1 and P2. All
355 rainfall indices were higher during the latter period than during the former period. Four extreme
356 indices (R95p, R99p, R95pF, and R99pF) were concentrated in July, August, and June. In P2,
357 this trend strengthened, showing reduced intensity in June (except for R99pF) and strengthening
358 in July and August. Owing to the larger increase in July, extreme precipitation appeared to
359 decrease in August. At the sub-seasonal scale, the precipitation core occurred at 30°N from early
360 to mid-June. Over time, it evolved and shifted to the KP. This core weakened from mid-July to
361 early August, but another precipitation signal reappeared near 30°N by mid-August. During P2,
362 this characteristic manifested with a stronger intensity of the major rainband and earlier timing.
363 In terms of long-term variations, we found that changes in the mean temperature and PRCPTOT
364 occurred at different times. The higher phase of the mean temperature, above the mean value,
365 was reached in the mid-2000s and stabilized in 2010. However, PRCPTOT achieved a higher
366 phase between the mid-1990s and 2010. Similarly, additional extreme precipitation indices, such
367 as RX1H, R95p, and R20mm, showed similar characteristics to PRCPTOT. The dry day had a
368 negative correlation with PRCPTOT. In other words, increases in the intensity and frequency of
369 extreme rainfall had a major impact on the total quantity of summer precipitation in recent years.
370 Moreover, PRCPTOT, RX1H, and R95p were elevated in urbanized regions.

371 Our results provided a foundation for understanding the mean and extreme precipitation
372 in South Korea in terms of trends, spatio-temporal variability, and long-term variation. First, we
373 emphasized the importance of observational data in the study of heavy rainfall. Second, extreme
374 rainfall had increased more than mean precipitation during the last five decades. In particular,
375 hourly-maximum precipitation increased significantly. Third, extreme precipitation played a
376 greater role in summer precipitation, and several extreme precipitation indices appeared higher in
377 urbanized areas. Finally, the intensification of the rainband occurred sooner over the recent two

378 decades. The results of this study suggested that extreme precipitation events would occur more
379 frequently and with greater intensity in the future. In the event of rapid and extreme rainfall, we
380 should be cautious and well-prepared.

381

382 **Acknowledgments**

383 This work was supported by a 2021-Year Culture Award Grant of Busan City. We acknowledge
384 Haeun Jeon and Woojin Jung for collecting data.

385

386 **Open Research**

387 ASOS data are downloadable from

388 <https://data.kma.go.kr/data/grnd/selectAsosRltmList.do?pgmNo=36>. ERA5 hourly data are

389 available at <https://cds.climate.copernicus.eu/cdsapp#!/dataset/reanalysis-era5-single->

390 [levels?tab=form](https://cds.climate.copernicus.eu/cdsapp#!/dataset/reanalysis-era5-single-levels?tab=form). ETOPO1 data can be found at <https://www.ncei.noaa.gov/products/etopo->

391 [global-relief-model](https://www.ncei.noaa.gov/products/etopo-global-relief-model).

392

393 **References**

- 394 Alexander, L. v., Zhang, X., Peterson, T. C., Caesar, J., Gleason, B., Klein Tank, A. M. G.,
395 Haylock, M., Collins, D., Trewin, B., Rahimzadeh, F., Tagipour, A., Rupa Kumar, K.,
396 Revadekar, J., Griffiths, G., Vincent, L., Stephenson, D. B., Burn, J., Aguilar, E., Brunet,
397 M., ... Vazquez-Aguirre, J. L. (2006). Global observed changes in daily climate extremes of
398 temperature and precipitation. *Journal of Geophysical Research Atmospheres*, *111*(5).
399 <https://doi.org/10.1029/2005JD006290>
- 400 Allan, R. P., & Soden, B. J. (2008). Atmospheric Warming and the Amplification of
401 Precipitation Extremes. *Science*, *321*(5895), 1481–1484.
402 <https://doi.org/10.1126/science.1107142>
- 403 Allen, M. R., & Ingram, W. J. (2002). Constraints on future changes in climate and the
404 hydrologic cycle. *Nature*. www.nature.com/nature
- 405 Amante, C., & Eakins, B. W. (2009). *NOAA Technical Memorandum NESDIS NGDC-24*
406 *ETOPO1 1 ARC-MINUTE GLOBAL RELIEF MODEL: PROCEDURES, DATA SOURCES*
407 *AND ANALYSIS*.

- 408 Azam, M., Maeng, S. J., Kim, H. S., Lee, S. W., & Lee, J. E. (2018). Spatial and temporal trend
 409 analysis of precipitation and drought in South Korea. *Water (Switzerland)*, *10*(6).
 410 <https://doi.org/10.3390/w10060765>
- 411 Bae, G., & Yeung, J. (2022, August 10). *Record rainfall kills at least 9 in Seoul as water floods*
 412 *buildings, submerges cars*. CNN.
- 413 Baek, H. J., Kim, M. K., & Kwon, W. T. (2017). Observed short- and long-term changes in
 414 summer precipitation over South Korea and their links to large-scale circulation anomalies.
 415 *International Journal of Climatology*, *37*(2), 972–986. <https://doi.org/10.1002/joc.4753>
- 416 Borodina, A., Fischer, E. M., & Knutti, R. (2017). Models are likely to underestimate increase in
 417 heavy rainfall in the extratropical regions with high rainfall intensity. *Geophysical Research*
 418 *Letters*, *44*(14), 7401–7409. <https://doi.org/10.1002/2017GL074530>
- 419 Chen, J.-M., & Harr, P. A. (1993). Interpretation of Extended Empirical Orthogonal Function
 420 (EEOF) Analysis. *Monthly Weather Review*, *121*, 2631–2636.
- 421 Chou, C., Chen, C. A., Tan, P. H., & Chen, K. T. (2012). Mechanisms for global warming
 422 impacts on precipitation frequency and intensity. *Journal of Climate*, *25*(9), 3291–3306.
 423 <https://doi.org/10.1175/JCLI-D-11-00239.1>
- 424 Dave, R., Subramanian, S. S., & Bhatia, U. (2021). Extreme precipitation induced concurrent
 425 events trigger prolonged disruptions in regional road networks. *Environmental Research*
 426 *Letters*, *16*(10). <https://doi.org/10.1088/1748-9326/ac2d67>
- 427 Ha, K. J., Moon, S., Timmermann, A., & Kim, D. (2020). Future Changes of Summer Monsoon
 428 Characteristics and Evaporative Demand Over Asia in CMIP6 Simulations. *Geophysical*
 429 *Research Letters*, *47*(8). <https://doi.org/10.1029/2020GL087492>
- 430 Ha, K. J., Yeo, J. H., Seo, Y. W., Chung, E. S., Moon, J. Y., Feng, X., Lee, Y. W., & Ho, C. H.
 431 (2020). What caused the extraordinarily hot 2018 summer in Korea? *Journal of the*
 432 *Meteorological Society of Japan*, *98*(1), 153–167. <https://doi.org/10.2151/jmsj.2020-009>
- 433 Ha, K.-J., & Oh, H. (2019). Multifaceted Intraseasonal Modes in the East Asian-Western North
 434 Pacific Summer Monsoon Climate. In *The Multiscale Global Monsoon System: Vol. Volume*
 435 *11* (pp. 37–47). WORLD SCIENTIFIC. https://doi.org/doi:10.1142/9789811216602_0004
- 436 Ha, K.-J., Yun, K.-S., Jhun, J.-G., & Li, J. (2009). Circulation changes associated with the
 437 interdecadal shift of Korean August rainfall around late 1960s. *Journal of Geophysical*
 438 *Research: Atmospheres*, *114*(D4). <https://doi.org/https://doi.org/10.1029/2008JD011287>
- 439 Held, I. M., & Soden, B. J. (2006). Robust Responses of the Hydrological Cycle to Global
 440 Warming. *Journal of Climate*, *19*(21), 5686–5699.
- 441 Hersbach, H., Bell, B., Berrisford, P., Hirahara, S., Horányi, A., Muñoz-Sabater, J., Nicolas, J.,
 442 Peubey, C., Radu, R., Schepers, D., Simmons, A., Soci, C., Abdalla, S., Abellan, X.,
 443 Balsamo, G., Bechtold, P., Biavati, G., Bidlot, J., Bonavita, M., ... Thépaut, J. N. (2020).
 444 The ERA5 global reanalysis. *Quarterly Journal of the Royal Meteorological Society*,
 445 *146*(730), 1999–2049. <https://doi.org/10.1002/qj.3803>
- 446 Ho, C. H., Lee, J. Y., Ahn, M. H., & Lee, H. S. (2003). A sudden change in summer rainfall
 447 characteristics in Korea during the late 1970s. *International Journal of Climatology*, *23*(1),
 448 117–128. <https://doi.org/10.1002/joc.864>
- 449 H.-O. Pörtner, D.C. Roberts, M. Tignor, E.S. Poloczanska, K. Mintenbeck, A. Alegría, M. Craig,
 450 S. Langsdorf, S. Löschke, v. Möller, A. Okem, & B. Rama. (2022). *IPCC, 2022: Climate*
 451 *Change 2022: Impacts, Adaptation, and Vulnerability. Contribution of Working Group II to*
 452 *the Sixth Assessment Report of the Intergovernmental Panel on Climate Change*.

- 453 Hu, W., Chen, L., Shen, J., Yao, J., He, Q., & Chen, J. (2022). Changes in Extreme Precipitation
454 on the Tibetan Plateau and Its Surroundings: Trends, Patterns, and Relationship with Ocean
455 Oscillation Factors. *Water*, 14(16). <https://doi.org/10.3390/w14162509>
- 456 Jeong, Y., Nam, S., Kwon, J.-I., Uppara, U., & Jo, Y.-H. (2022). Surface Warming Slowdown
457 With Continued Subsurface Warming in the East Sea (Japan Sea) Over Recent Decades
458 (2000–2014). *Frontiers in Marine Science*, 9. <https://doi.org/10.3389/fmars.2022.825368>
- 459 Jia, Z., Zheng, Z., Feng, G., & Tong, M. (2022). The Intraseasonal Variations of the Leading
460 Mode of Summer Precipitation Anomalies in Meiyu Area of East Asia. *Atmosphere*, 13(2).
461 <https://doi.org/10.3390/atmos13020217>
- 462 Jung, H. S., Choi, Y., Oh, J. H., & Lim, G. H. (2002). Recent trends in temperature and
463 precipitation over South Korea. *International Journal of Climatology*, 22(11), 1327–1337.
464 <https://doi.org/10.1002/joc.797>
- 465 Jung, I. W., Bae, D. H., & Kim, G. (2011). Recent trends of mean and extreme precipitation in
466 Korea. *International Journal of Climatology*, 31(3), 359–370.
467 <https://doi.org/10.1002/joc.2068>
- 468 Kharin, V. v., Zwiers, F. W., Zhang, X., & Hegerl, G. C. (2007). Changes in temperature and
469 precipitation extremes in the IPCC ensemble of global coupled model simulations. *Journal*
470 *of Climate*, 20(8), 1419–1444. <https://doi.org/10.1175/JCLI4066.1>
- 471 Kim, H., Lee, J.-H., Park, H.-J., & Heo, J.-H. (2021). Assessment of temporal probability for
472 rainfall-induced landslides based on nonstationary extreme value analysis. *Engineering*
473 *Geology*, 294. <https://doi.org/https://doi.org/10.1016/j.enggeo.2021.106372>
- 474 Kim, J., Choi, J., Choi, C., & Park, S. (2013). Impacts of changes in climate and land use/land
475 cover under IPCC RCP scenarios on streamflow in the Hoeya River Basin, Korea. *Science*
476 *of the Total Environment*, 452–453, 181–195.
477 <https://doi.org/10.1016/j.scitotenv.2013.02.005>
- 478 Kim, J. H., Wu, C. C., Sui, C. H., & Ho, C. H. (2012). Tropical cyclone contribution to
479 interdecadal change in summer rainfall over South China in the early 1990s. *Terrestrial,*
480 *Atmospheric and Oceanic Sciences*, 23(1), 49–58.
481 [https://doi.org/10.3319/TAO.2011.08.26.01\(A\)](https://doi.org/10.3319/TAO.2011.08.26.01(A))
- 482 Kim, K. Y., Kitoh, A., & Ha, K. J. (2008). The SST-forced predictability of the sub-seasonal
483 mode over East Asia with an atmospheric general circulation model. *International Journal*
484 *of Climatology*, 28(12), 1599–1606. <https://doi.org/10.1002/joc.1655>
- 485 Kim, S., & Ha, K.-J. (2021). Interannual and decadal covariabilities in East Asian and Western
486 North Pacific summer rainfall for 1979–2016. *Climate Dynamics*, 56(3), 1017–1033.
487 <https://doi.org/10.1007/s00382-020-05517-7>
- 488 Korea Meteorological Administration. (2020). *Korean Climage Change Assessment Report*
489 *2020-The Physical Science Basis-Summary for Policymakers*.
- 490 Lee, J.-Y., Kwon, M., Yun, K.-S., Min, S.-K., Park, I.-H., Ham, Y.-G., Jin, E. K., Kim, J.-H.,
491 Seo, K.-H., Kim, W., Yim, S.-Y., & Yoon, J.-H. (2017). The long-term variability of
492 Changma in the East Asian summer monsoon system: A review and revisit. *Asia-Pacific*
493 *Journal of Atmospheric Sciences*, 53(2), 257–272. [https://doi.org/10.1007/s13143-017-](https://doi.org/10.1007/s13143-017-0032-5)
494 [0032-5](https://doi.org/10.1007/s13143-017-0032-5)
- 495 Lee, M. H., Ho, C. H., Kim, J., & Song, C. K. (2012). Assessment of the changes in extreme
496 vulnerability over East Asia due to global warming. *Climatic Change*, 113(2), 301–321.
497 <https://doi.org/10.1007/s10584-011-0345-9>

- 498 Meyer, J., Neuper, M., Mathias, L., Zehe, E., & Pfister, L. (2021). More frequent flash flood
499 events and extreme precipitation favouring atmospheric conditions in temperate regions of
500 Europe. *Hydrology and Earth System Sciences*. <https://doi.org/10.5194/hess-2021-628>
- 501 Min, S. K., Son, S. W., Seo, K. H., Kug, J. S., An, S. il, Choi, Y. S., Jeong, J. H., Kim, B. M.,
502 Kim, J. W., Kim, Y. H., Lee, J. Y., & Lee, M. I. (2015). Changes in weather and climate
503 extremes over Korea and possible causes: A review. In *Asia-Pacific Journal of Atmospheric*
504 *Sciences* (Vol. 51, Issue 2, pp. 103–121). Korean Meteorological Society.
505 <https://doi.org/10.1007/s13143-015-0066-5>
- 506 Min, S. K., Zhang, X., Zwiers, F. W., & Hegerl, G. C. (2011). Human contribution to more-
507 intense precipitation extremes. *Nature*, *470*(7334), 378–381.
508 <https://doi.org/10.1038/nature09763>
- 509 Moberg, A., Jones, P. D., Lister, D., Walther, A., Brunet, M., Jacobeit, J., Alexander, L. v, Della-
510 Marta, P. M., Luterbacher, J., Yiou, P., Chen, D., Tank, A. M. G. K., Saladié, O., Sigró, J.,
511 Aguilar, E., Alexandersson, H., Almarza, C., Auer, I., Barriendos, M., ... Xoplaki, E.
512 (2006). Indices for daily temperature and precipitation extremes in Europe analyzed for the
513 period 1901–2000. *Journal of Geophysical Research: Atmospheres*, *111*(D22).
514 <https://doi.org/https://doi.org/10.1029/2006JD007103>
- 515 Moon, M., & Ha, K. J. (2021). Abnormal Activities of Tropical Cyclones in 2019 Over the
516 Korean Peninsula. *Geophysical Research Letters*, *48*(7).
517 <https://doi.org/10.1029/2020GL090784>
- 518 Ning, G., Luo, M., Zhang, Q., Wang, S., Liu, Z., Yang, Y., Wu, S., & Zeng, Z. (2021).
519 Understanding the Mechanisms of Summer Extreme Precipitation Events in Xinjiang of
520 Arid Northwest China. *Journal of Geophysical Research: Atmospheres*, *126*(15).
521 <https://doi.org/10.1029/2020JD034111>
- 522 O’Gorman, P. A., & Schneider, T. (2009). The physical basis for increases in precipitation
523 extremes in simulations of 21st-century climate change. *Proceedings of the National*
524 *Academy of Sciences of the United States of America*, *106*(35), 14773–14777.
525 <https://doi.org/10.1073/pnas.0907610106>
- 526 Park, B. J., Kim, Y. H., Min, S. K., Kim, M. K., Choi, Y., Boo, K. O., & Shim, S. (2017). Long-
527 Term Warming Trends in Korea and Contribution of Urbanization: An Updated
528 Assessment. *Journal of Geophysical Research: Atmospheres*, *122*(20), 10,637–10,654.
529 <https://doi.org/10.1002/2017JD027167>
- 530 Park, C., Son, S.-W., Kim, H., Ham, Y.-G., Kim, J., Cha, D.-H., Chang, E.-C., Lee, G., Kug, J.-
531 S., Lee, W.-S., Lee, Y.-Y., Lee, H. C., & Lim, B. (2021). Record-Breaking Summer
532 Rainfall in South Korea in 2020: Synoptic Characteristics and the Role of Large-Scale
533 Circulations. *Monthly Weather Review*, *149*, 3085–3100. <https://doi.org/10.1175/MWR-D>
- 534 Park, H. L., Seo, K. H., & Son, J. H. (2015). Development of a dynamics-based statistical
535 prediction model for the Changma onset. *Journal of Climate*, *28*(17), 6647–6666.
536 <https://doi.org/10.1175/JCLI-D-14-00502.1>
- 537 Pei, L., Xia, J., Yan, Z., & Yang, H. (2017). Assessment of the Pacific decadal oscillation’s
538 contribution to the occurrence of local torrential rainfall in north China. *Climatic Change*,
539 *144*(3), 391–403. <https://doi.org/10.1007/s10584-016-1610-8>
- 540 Ren, Q., Liu, F., Wang, B., Yang, S., Wang, H., & Dong, W. (2022). Origins of the Intraseasonal
541 Variability of East Asian Summer Precipitation. *Geophysical Research Letters*, *49*(4).
542 <https://doi.org/10.1029/2021GL096574>

- 543 Ryan, C., Curley, M., Walsh, S., & Murphy, C. (2022). Long-term trends in extreme
544 precipitation indices in Ireland. *International Journal of Climatology*, *42*(7), 4040–4061.
545 <https://doi.org/https://doi.org/10.1002/joc.7475>
- 546 Seo, K.-H., Son, J.-H., & Lee, J.-Y. (2011). A New Look at Changma. *Atmosphere*, *21*, 109–121.
- 547 Seo, Y. W., Ha, K. J., & Park, T. W. (2021). Feedback attribution to dry heatwaves over East
548 Asia. *Environmental Research Letters*, *16*(6). <https://doi.org/10.1088/1748-9326/abf18f>
- 549 Soon-il, A., Kyung-Ja, H., Kyong-Hwan, S., Sang-Wook, Y., Seung-Ki, M., & Chang-Hoi, H.
550 (2011). A Review of Recent Climate Trends and Causes over the Korean Peninsula. *Journal*
551 *of Climate Change Research(한국기후변화학회지)*, *2*(4), 237–251. www.dbpia.co.kr
- 552 Trenberth, K. E., Dai, A., Rasmussen, R. M., & Parsons, D. B. (2003). THE CHANGING
553 CHARACTER OF PRECIPITATION. *Bulletin of the American Meteorological Society*,
554 *84*(9), 1205–1218.
- 555 Wang, B., Biasutti, M., Byrne, M. P., Castro, C., Chang, C.-P., Cook, K., Fu, R., Grimm, A. M.,
556 Ha, K.-J., Hendon, H., Kitoh, A., Krishnan, R., Lee, J.-Y., Li, J., Liu, J., Moise, A., Pascale,
557 S., Roxy, M. K., Seth, A., ... Zhou, T. (2021). Monsoons Climate Change Assessment.
558 *Bulletin of the American Meteorological Society*, *102*(1), E1–E19.
559 <https://doi.org/10.1175/BAMS-D-19-0335.1>
- 560 Wu, Z., & Huang, N. E. (2004). A study of the characteristics of white noise using the empirical
561 mode decomposition method. *Proceedings of the Royal Society of London. Series A:*
562 *Mathematical, Physical and Engineering Sciences*, *460*(2046), 1597–1611.
563 <https://doi.org/10.1098/rspa.2003.1221>
- 564 Wu, Z., & Huang, N. E. (2009). Ensemble empirical mode decomposition: a noise-assisted data
565 analysis method. *Advances in Adaptive Data Analysis*, *01*(01), 1–41.
566 <https://doi.org/10.1142/S1793536909000047>
- 567 Yao, C., Yang, S., Qian, W., Lin, Z., & Wen, M. (2008). Regional summer precipitation events
568 in Asia and their changes in the past decades. *Journal of Geophysical Research*
569 *Atmospheres*, *113*(17). <https://doi.org/10.1029/2007JD009603>
- 570 Yun, J., Ha, K.-J., & Jo, Y.-H. (2018). Interdecadal changes in winter surface air temperature
571 over East Asia and their possible causes. *Climate Dynamics*, *51*(4), 1375–1390.
572 <https://doi.org/10.1007/s00382-017-3960-y>

573

574